# Higher-Order Finite Element Schemes for Compressible Flow [1]

Miloslav Feistauer and Vít Dolejší
Charles University Prague

**Goal:**
to develop a sufficiently accurate and robust method for the numerical simulation of compressible flow

## 1 Continuous problem

$\Omega \subset I\!R^N$ a bounded domain and $T > 0$.
$Q_T = \Omega \times (0, T)$
$\partial\Omega$ consists of several disjoint parts:
inlet $\Gamma_I$
outlet $\Gamma_O$
impermeable walls $\Gamma_W$ on $\partial\Omega$

[1]Presented at the Winter School ENVIRONMENTAL AND INDUSTRIAL CFD SIMULATIONS, Prague, 24 February 2004.
This work was supported under the Grant No. 201/02/0684 of the Czech Grant Agency and the Grant No. MSM 113200007 of the Ministry of Education of the Czech Republic.

**Basic equations:** *continuity eq., Navier-Stokes eq's, energy equation*

$$\frac{\partial \boldsymbol{w}}{\partial t} + \sum_{s=1}^{N} \frac{\partial \boldsymbol{f}_s(\boldsymbol{w})}{\partial x_s} = \sum_{s=1}^{N} \frac{\partial \boldsymbol{R}_s(\boldsymbol{w}, \nabla \boldsymbol{w})}{\partial x_s} \quad \text{in } Q_T, \tag{1.1}$$

$$\begin{aligned} \boldsymbol{w} &= (\rho, \rho v_1, \ldots, \rho v_N, E)^{\mathrm{T}} \in I\!R^m, \\ \boldsymbol{w} &= \boldsymbol{w}(x,t),\ x \in \Omega,\ t \in (0,T), \\ \boldsymbol{f}_i(\boldsymbol{w}) &= (f_{i1}, \ldots, f_{im})^{\mathrm{T}} \\ &= (\rho v_i, \rho v_1 v_i + \delta_{1i}\, p, \ldots, \rho v_N v_i + \delta_{Ni}\, p, (E+p) v_i)^{\mathrm{T}} \\ \boldsymbol{R}_i(\boldsymbol{w}, \nabla \boldsymbol{w}) &= (R_{i1}, \ldots, R_{im})^{\mathrm{T}} \\ &= (0, \tau_{i1}, \ldots, \tau_{iN}, \tau_{i1}\, v_1 + \cdots + \tau_{iN}\, v_N + k\partial\theta/\partial x_i)^{\mathrm{T}}, \\ \tau_{ij} &= \lambda\, \mathrm{div} \boldsymbol{v} \delta_{ij} + 2\mu\, d_{ij}(\boldsymbol{v}),\ d_{ij}(\boldsymbol{v}) = \frac{1}{2}\left(\frac{\partial v_i}{\partial x_j} + \frac{\partial v_j}{\partial x_i}\right). \end{aligned} \tag{1.2}$$

*Thermodynamical relations:*

$$p = (\gamma - 1)(E - \rho |\boldsymbol{v}|^2/2), \quad \theta = \left(\frac{E}{\rho} - \frac{1}{2}|\boldsymbol{v}|^2\right)/c_v. \tag{1.3}$$

*Notation*:
$\boldsymbol{v} = (v_1, \ldots, v_N)^{\mathrm{T}}$ – velocity vector
$\rho$ – density
$p$ – pressure
$\theta$ – absolute temperature
$E$ – total energy
$\gamma$ – Poisson adiabatic constant, $c_v$ – specific heat at constant volume, $\mu, \lambda$ – viscosity coefficients, $k$ – heat conduction coefficient
We assume $\mu, k > 0$ and set $\lambda = -2\mu/3$.

**Initial condition:**

$$\boldsymbol{w}(x,0) = \boldsymbol{w}^0(x), \quad x \in \Omega, \tag{1.4}$$

**Boundary conditions:**

$$\text{a)}\ \ \rho|_{\Gamma_I\times(0,T)} = \rho_D, \tag{1.5}$$
$$\text{b)}\ \ \boldsymbol{v}|_{\Gamma_I\times(0,T)} = \boldsymbol{v}_D = (v_{D1},\dots,v_{DN})^{\mathrm{T}},$$
$$\text{c)}\ \ \sum_{j=1}^{N}\left(\sum_{i=1}^{N}\tau_{ij}n_i\right)v_j + k\,\frac{\partial\theta}{\partial n} = 0 \quad \text{on } \Gamma_I\times(0,T);$$
$$\text{a)}\ \ \boldsymbol{v}|_{\Gamma_W\times(0,T)} = 0, \tag{1.6}$$
$$\text{b)}\ \ \frac{\partial\theta}{\partial n}|_{\Gamma_W\times(0,T)} = 0 \quad \text{on } \Gamma_W\times(0,T);$$
$$\text{a)}\sum_{i=1}^{N}\tau_{ij}n_i = 0, \quad j = 1,\dots,N, \tag{1.7}$$
$$\text{b)}\frac{\partial\theta}{\partial n} = 0 \quad \text{on } \Gamma_O\times(0,T)$$

**Inviscid limit:**

$\mu = \lambda = k = 0$ then $\boldsymbol{R}_s \equiv 0,\ s = 1,\dots,N$ in (1.1): we obtain the system of the Euler equations describing a motion of inviscid compressible fluids, equipped with *"inviscid" boundary conditions*: local 1D initial-boundary value Riemann problem in the direction $\boldsymbol{n}$ – linearly well-posed.

**Problem (CFP):** to solve the compressible Navier–Stokes equations,

**Problem (iCFP):** to solve the inviscid compressible Euler equations

**Numerical solution of compressible flow = one of the most difficult problems of CFD**

**Obstacles:**

hyperbolic – parabolic character of equations
convection dominating over diffusion ($\mu, \lambda, k$ small)
shock waves, contact discontinuities
boundary layers, wakes
lack of theory for the continuous problem

## 2 Discretization

### Wide spread meaning in CFD:

**FEM** suitable for diffusion and elasticity problems

**FVM** adequate for convection-diffusion problems of fluid dynamics

*advantage of FVM*: discontinuous approximate solution

*disadvantage of FVM*: low order of accuracy and its problematic increase

**Compromise** between FEM and FVM = **DGFEM**:
piecewise polynomial approximations,
no continuity requirement on interfaces between neighbouring elements

## DGFE discretization

$\Omega_h$ – polygonal approximation of the domain $\Omega$

$\mathcal{T}_h = \{K_i\}_{i \in I}$ $(h > 0)$ – standard triangulation of $\overline{\Omega}_h$

$I \subset Z^+ = \{0, 1, 2, \ldots\}$ is a suitable index set

$h_K = \mathrm{diam}(K)$, $h = \max_{K \in \mathcal{T}_h} h_K$

If two elements $K_i$, $K_j \in \mathcal{T}_h$ have a common interface $\Gamma_{ij}$, we call them *neighbours*.

For $i \in I$ we set $s(i) = \{j \in I; K_j \text{ is a neighbour of } K_i\}$.

Boundary faces: also denoted by $\Gamma_{ij}$ = face of $K_i$ adjacent to $\partial\Omega_h$, for $j \in \gamma(i)$.

For $K_i$ not adjacent to $\partial\Omega_h$ we set $\gamma(i) = \emptyset$.

$S(i) = s(i) \cup \gamma(i) \Longrightarrow$.

$$\partial K_i = \bigcup_{j \in S(i)} \Gamma_{ij}, \qquad \partial K_i \cap \partial\Omega_h = \bigcup_{j \in \gamma(i)} \Gamma_{ij}. \tag{2.8}$$

**Further notation**:

$\boldsymbol{n}_{ij} = ((n_{ij})_1, \ldots, (n_{ij})_N)$ = unit outer normal to $\partial K_i$ on the face $\Gamma_{ij}$ ($\boldsymbol{n}_{ij}$ is a constant vector on $\Gamma_{ij}$),
$d(\Gamma_{ij}) = \mathrm{diam}(\Gamma_{ij})$

$\gamma_D(i)$ = subset of $\gamma(i)$ formed by such indexes $j$ that the faces $\Gamma_{ij}$ approximate the parts of $\partial\Omega$, where some Dirichlet boundary condition is prescribed $\Longrightarrow$

$$\bigcup_{i\in I}\bigcup_{j\in\gamma_D(i)}\Gamma_{ij} = \Gamma_I \cup \Gamma_W. \tag{2.9}$$

Moreover, we set

$$\gamma_N(i) = \gamma(i) \setminus \gamma_D(i) \tag{2.10}$$

**Broken Sobolev space**:

$$H^k(\Omega_h, \mathcal{T}_h) = \{v; v|_K \in H^k(K)\ \forall\, K \in \mathcal{T}_h\}. \tag{2.11}$$

For $v \in H^1(\Omega_h, \mathcal{T}_h)$ we set

$$\begin{aligned} \langle v\rangle_{\Gamma_{ij}} &= \frac{1}{2}\left(v|_{\Gamma_{ij}} + v|_{\Gamma_{ji}}\right), \\ [v]_{\Gamma_{ij}} &= v|_{\Gamma_{ij}} - v|_{\Gamma_{ji}}, \end{aligned} \tag{2.12}$$

= *average* and *jump of the traces* of $v$ on $\Gamma_{ij} = \Gamma_{ji}$.

## Approximate DG solution

The approximate solution $\boldsymbol{w}_h$ is sought in

$$\boldsymbol{S}_h = [S_h]^m, \tag{2.13}$$

$$S_h = S^{p,-1}(\Omega, \mathcal{T}_h) = \{v; v|_K \in P^p(K)\ \forall\, K \in \mathcal{T}_h\}, \tag{2.14}$$

$P^p(K)$ = the space of all polynomials on $K$ of degree $\leq p$.

## Derivation of the discrete problem

## I) "Weak formulation"

Assume that $\boldsymbol{w}$ is a classical sufficiently regular solution of the Navier-Stokes equations and $\boldsymbol{\varphi} \in H^2(\Omega_h, \mathcal{T}_h)^m$

Multiply equation (1.1) by $\boldsymbol{\varphi}$

Integrate over $K_i \in \mathcal{T}_h$

Apply Green's theorem

Sum over all $K_i \in \mathcal{T}_h$ and rearrange

Use natural Neumann conditions $\Longrightarrow$

$$
\begin{aligned}
(2.15) \quad & \int_\Omega \frac{\partial \boldsymbol{w}}{\partial t} \cdot \boldsymbol{\varphi} \, \mathrm{d}x \\
& + \sum_{i \in I} \sum_{j \in S(i)} \int_{\Gamma_{ij}} \sum_{s=1}^{N} \boldsymbol{f}_s(\boldsymbol{w}) \, (n_{ij})_s \cdot \boldsymbol{\varphi}|_{\Gamma_{ij}} \mathrm{d}S \\
& - \sum_{i \in I} \int_{K_i} \sum_{s=1}^{N} \boldsymbol{f}_s(\boldsymbol{w}) \cdot \frac{\partial \boldsymbol{\varphi}}{\partial x_s} \, \mathrm{d}x \\
& + \sum_{i \in I} \int_{K_i} \sum_{s=1}^{N} \boldsymbol{R}_s(\boldsymbol{w}, \nabla \boldsymbol{w}) \cdot \frac{\partial \boldsymbol{\varphi}}{\partial x_s} \, \mathrm{d}x \\
& \quad - \sum_{i \in I} \sum_{\substack{j \in s(i) \\ j < i}} \int_{\Gamma_{ij}} \sum_{s=1}^{N} \langle \boldsymbol{R}_s(\boldsymbol{w}, \nabla \boldsymbol{w}) \rangle \, (n_{ij})_s \cdot [\boldsymbol{\varphi}] \, \mathrm{d}S \\
& \quad - \sum_{i \in I} \sum_{j \in \gamma_D(i)} \int_{\Gamma_{ij}} \sum_{s=1}^{N} \boldsymbol{R}_s(\boldsymbol{w}, \nabla \boldsymbol{w}) \, (n_{ij})_s \cdot \boldsymbol{\varphi} \, \mathrm{d}S = 0.
\end{aligned}
$$

## II) Stabilization

*a) Viscous terms:*
Add to (2.15) suitable terms which vanish for a smooth solution $\boldsymbol{w}$ or mutually cancel

**Partial linearization of the viscous terms $\boldsymbol{R}_s(\boldsymbol{w}, \nabla \boldsymbol{w})$:**
For example, if $N = 2$, from (1.2) we obtain

$$\boldsymbol{R}_1(\boldsymbol{w}, \nabla \boldsymbol{w})$$
$$= \begin{pmatrix} 0 \\ \frac{2}{3}\frac{\mu}{w_1}\left[2\left(\frac{\partial w_2}{\partial x_1} - \frac{w_2}{w_1}\frac{\partial w_1}{\partial x_1}\right) - \left(\frac{\partial w_3}{\partial x_2} - \frac{w_3}{w_1}\frac{\partial w_1}{\partial x_2}\right)\right] \\ \frac{\mu}{w_1}\left[\left(\frac{\partial w_3}{\partial x_1} - \frac{w_3}{w_1}\frac{\partial w_1}{\partial x_1}\right) + \left(\frac{\partial w_2}{\partial x_2} - \frac{w_2}{w_1}\frac{\partial w_1}{\partial x_2}\right)\right] \\ \frac{w_2}{w_1}\boldsymbol{R}_1^{(2)} + \frac{w_3}{w_1}\boldsymbol{R}_1^{(3)} + \frac{k}{c_v w_1}\Big[\frac{\partial w_4}{\partial x_1} - \frac{w_4}{w_1}\frac{\partial w_1}{\partial x_1} - \frac{1}{w_1}\left(w_2\frac{\partial w_2}{\partial x_1} + w_3\frac{\partial w_3}{\partial x_1}\right) \\ \qquad + \frac{1}{w_1^2}\left(w_2^2 + w_3^2\right)\frac{\partial w_1}{\partial x_1}\Big] \end{pmatrix},$$

$$\boldsymbol{R}_2(\boldsymbol{w}, \nabla \boldsymbol{w})$$
$$= \begin{pmatrix} 0 \\ \frac{\mu}{w_1}\left[\left(\frac{\partial w_3}{\partial x_1} - \frac{w_3}{w_1}\frac{\partial w_1}{\partial x_1}\right) + \left(\frac{\partial w_2}{\partial x_2} - \frac{w_2}{w_1}\frac{\partial w_1}{\partial x_2}\right)\right] \\ \frac{2}{3}\frac{\mu}{w_1}\left[2\left(\frac{\partial w_3}{\partial x_2} - \frac{w_3}{w_1}\frac{\partial w_1}{\partial x_2}\right) - \left(\frac{\partial w_2}{\partial x_1} - \frac{w_2}{w_1}\frac{\partial w_1}{\partial x_1}\right)\right] \\ \frac{w_2}{w_1}\boldsymbol{R}_2^{(2)} + \frac{w_3}{w_1}\boldsymbol{R}_2^{(3)} + \frac{k}{c_v w_1}\Big[\frac{\partial w_4}{\partial x_1} - \frac{w_4}{w_1}\frac{\partial w_1}{\partial x_2} - \frac{1}{w_1}\left(w_2\frac{\partial w_2}{\partial x_2} + w_3\frac{\partial w_3}{\partial x_2}\right) \\ \qquad + \frac{1}{w_1^2}\left(w_2^2 + w_3^2\right)\frac{\partial w_1}{\partial x_2}\Big] \end{pmatrix},$$

where $\boldsymbol{R}_s^{(r)} = \boldsymbol{R}_s^{(r)}(\boldsymbol{w}, \nabla \boldsymbol{w})$ denotes the $r$-th component of $\boldsymbol{R}_s$ $(s = 1, 2,\ r = 2, 3)$.

Now for $\boldsymbol{w} = (w_1, \dots, w_4)^{\mathrm{T}}$ and $\boldsymbol{\varphi} = (\varphi_1, \dots, \varphi_4)^{\mathrm{T}}$ we define the vector-valued functions

$$
\begin{aligned}
&\boldsymbol{D}_1(\boldsymbol{w}, \nabla \boldsymbol{w}, \boldsymbol{\varphi}, \nabla \boldsymbol{\varphi}) \\
&= \begin{pmatrix}
0 \\
\frac{2}{3}\,\frac{\mu}{w_1}\left[2\left(\frac{\partial \varphi_2}{\partial x_1} - \frac{\varphi_2}{w_1}\frac{\partial w_1}{\partial x_1}\right) - \left(\frac{\partial \varphi_3}{\partial x_2} - \frac{\varphi_3}{w_1}\frac{\partial w_1}{\partial x_2}\right)\right] \\
\frac{\mu}{w_1}\left[\left(\frac{\partial \varphi_3}{\partial x_1} - \frac{\varphi_3}{w_1}\frac{\partial w_1}{\partial x_1}\right) + \left(\frac{\partial \varphi_2}{\partial x_2} - \frac{\varphi_2}{w_1}\frac{\partial w_1}{\partial x_2}\right)\right] \\
\frac{w_2}{w_1}\boldsymbol{D}_1^{(2)} + \frac{w_3}{w_1}\boldsymbol{D}_1^{(3)} + \frac{k}{c_v w_1}\Big[\frac{\partial \varphi_4}{\partial x_1} - \frac{\varphi_4}{w_1}\frac{\partial w_1}{\partial x_1} - \frac{1}{w_1}\left(w_2\frac{\partial \varphi_2}{\partial x_1} + w_3\frac{\partial \varphi_3}{\partial x_1}\right) \\
\hfill + \frac{1}{w_1^2}\left(w_2\varphi_2 + w_3\varphi_3\right)\frac{\partial w_1}{\partial x_1}\Big]
\end{pmatrix},
\end{aligned}
$$

$$
\begin{aligned}
&\boldsymbol{D}_2(\boldsymbol{w}, \nabla \boldsymbol{w}, \boldsymbol{\varphi}, \nabla \boldsymbol{\varphi}) \\
&= \begin{pmatrix}
0 \\
\frac{\mu}{w_1}\left[\left(\frac{\partial \varphi_3}{\partial x_1} - \frac{\varphi_3}{w_1}\frac{\partial w_1}{\partial x_1}\right) + \left(\frac{\partial \varphi_2}{\partial x_2} - \frac{\varphi_2}{w_1}\frac{\partial w_1}{\partial x_2}\right)\right] \\
\frac{2}{3}\,\frac{\mu}{w_1}\left[2\left(\frac{\partial \varphi_3}{\partial x_2} - \frac{\varphi_2}{w_1}\frac{\partial w_1}{\partial x_2}\right) - \left(\frac{\partial \varphi_2}{\partial x_1} - \frac{\varphi_2}{w_1}\frac{\partial w_1}{\partial x_1}\right)\right] \\
\frac{w_2}{w_1}\boldsymbol{D}_2^{(2)} + \frac{w_3}{w_1}\boldsymbol{D}_2^{(3)} + \frac{k}{c_v w_1}\Big[\frac{\partial \varphi_4}{\partial x_2} - \frac{\varphi_4}{w_1}\frac{\partial w_1}{\partial x_2} - \frac{1}{w_1}\left(w_2\frac{\partial \varphi_2}{\partial x_2} + w_2\frac{\partial \varphi_3}{\partial x_2}\right) \\
\hfill + \frac{1}{w_1^2}\left(w_2\varphi_2 + w_3\varphi_3\right)\frac{\partial w_1}{\partial x_2}\Big]
\end{pmatrix},
\end{aligned}
$$

$\boldsymbol{D}_s^{(r)}$ denotes the $r$-th component of $\boldsymbol{D}_s$ $(s = 1, 2,\ r = 2, 3)$.

$\boldsymbol{D}_1$ and $\boldsymbol{D}_2$ – linear with respect to $\boldsymbol{\varphi}$ and $\nabla\boldsymbol{\varphi}$ and

$$
\boldsymbol{D}_s(\boldsymbol{w}, \nabla \boldsymbol{w}, \boldsymbol{w}, \nabla \boldsymbol{w}) = \boldsymbol{R}_s(\boldsymbol{w}, \nabla \boldsymbol{w}), \quad s = 1, 2. \tag{2.16}
$$

(Similarly we can proceed in the 3D case $(N = 3)$.)

We add the following terms to the left-hand side of (2.15):

$$\sum_{i\in I}\sum_{\substack{j\in s(i)\\ j<i}}\int_{\Gamma_{ij}}\sum_{s=1}^{N}\langle \boldsymbol{D}_s(\boldsymbol{w},\nabla\boldsymbol{w},\boldsymbol{\varphi},\nabla\boldsymbol{\varphi})\rangle\,(n_{ij})_s\;\cdot[\boldsymbol{w}]\,\mathrm{d}S$$
$$+\sum_{i\in I}\sum_{j\in\gamma_D(i)}\int_{\Gamma_{ij}}\sum_{s=1}^{N}\boldsymbol{D}_s(\boldsymbol{w},\nabla\boldsymbol{w},\boldsymbol{\varphi},\nabla\boldsymbol{\varphi})\,(n_{ij})_s\;\cdot\boldsymbol{w}\,\mathrm{d}S.$$

In the second term the Dirichlet conditions are taken into account with the aid of additional terms on the right-hand side of (2.15).

$\Longrightarrow$ *Nonsymmetric formulation of the viscous terms:*

$$\begin{aligned}
&a_h(\boldsymbol{w},\boldsymbol{\varphi})\\
=\;&\sum_{i\in I}\int_{K_i}\sum_{s=1}^{N}\boldsymbol{R}_s(\boldsymbol{w},\nabla\boldsymbol{w})\cdot\frac{\partial\boldsymbol{\varphi}}{\partial x_s}\,\mathrm{d}x\\
&\quad-\sum_{i\in I}\sum_{\substack{j\in s(i)\\ j<i}}\int_{\Gamma_{ij}}\sum_{s=1}^{N}\langle\boldsymbol{R}_s(\boldsymbol{w},\nabla\boldsymbol{w})\rangle\,(n_{ij})_s\cdot[\boldsymbol{\varphi}]\,\mathrm{d}S\\
&\quad+\sum_{i\in I}\sum_{\substack{j\in s(i)\\ j<i}}\int_{\Gamma_{ij}}\sum_{s=1}^{N}\langle\boldsymbol{D}_s(\boldsymbol{w},\nabla\boldsymbol{w},\boldsymbol{\varphi},\nabla\boldsymbol{\varphi})\rangle\,(n_{ij})_s\cdot[\boldsymbol{w}]\,\mathrm{d}S\\
&\quad-\sum_{i\in I}\sum_{j\in\gamma_D(i)}\int_{\Gamma_{ij}}\sum_{s=1}^{N}\boldsymbol{R}_s(\boldsymbol{w},\nabla\boldsymbol{w})\,(n_{ij})_s\cdot\boldsymbol{\varphi}\,\mathrm{d}S\\
&\quad+\sum_{i\in I}\sum_{j\in\gamma_D(i)}\int_{\Gamma_{ij}}\sum_{s=1}^{N}\boldsymbol{D}_s(\boldsymbol{w},\nabla\boldsymbol{w},\boldsymbol{\varphi},\nabla\boldsymbol{\varphi})\,(n_{ij})_s\,\boldsymbol{w}\,\mathrm{d}S
\end{aligned}$$

*b) Interior and boundary penalty terms*

To the left-hand side of (2.15) we add the vanishing *interior penalty* terms

$$\sum_{i\in I}\sum_{\substack{j\in s(i)\\ j<i}}\int_{\Gamma_{ij}}\sigma[\boldsymbol{w}]\cdot[\boldsymbol{\varphi}]\,\mathrm{d}S \tag{2.17}$$

and *boundary penalty terms*

$$\sum_{i\in I}\sum_{j\in\gamma_D(i)}\int_{\Gamma_{ij}}\sigma\boldsymbol{w}\cdot\boldsymbol{\varphi}\,\mathrm{d}S \tag{2.18}$$

with $\sigma|_{\Gamma_{ij}} = \mu/d(\Gamma_{ij})$

balanced by additional right-hand side terms containing the Dirichlet boundary data

$\Longrightarrow$ *Penalty form*

$$J_h(\boldsymbol{w},\boldsymbol{\varphi}) = \sum_{i\in I}\sum_{\substack{j\in s(i)\\ j<i}}\int_{\Gamma_{ij}}\sigma[\boldsymbol{w}]\cdot[\boldsymbol{\varphi}]\mathrm{d}S + \sum_{i\in I}\sum_{j\in\gamma_D(i)}\int_{\Gamma_{ij}}\sigma\,\boldsymbol{w}\cdot\boldsymbol{\varphi}\,\mathrm{d}S$$

*c) Right-hand side form*

$$\begin{aligned}\beta_h(\boldsymbol{w},\boldsymbol{\varphi}) \;=\; & \sum_{i\in I}\sum_{j\in\gamma_D(i)}\int_{\Gamma_{ij}}\sum_{s=1}^{N}\boldsymbol{D}_s(\boldsymbol{w},\nabla\boldsymbol{w},\boldsymbol{\varphi},\nabla\boldsymbol{\varphi})\,(n_{ij})_s\cdot\boldsymbol{w}_B\,\mathrm{d}S\\ & +\sum_{i\in I}\sum_{j\in\gamma_D(i)}\int_{\Gamma_{ij}}\sigma\,\boldsymbol{w}_B\cdot\boldsymbol{\varphi}\,\mathrm{d}S\end{aligned}$$

The boundary state $\boldsymbol{w}_B$ will be defined later.

Finally, we put

$$\boldsymbol{A}_h(\boldsymbol{w},\boldsymbol{\varphi}) = a_h(\boldsymbol{w},\boldsymbol{\varphi}) + J_h(\boldsymbol{w},\boldsymbol{\varphi}) - \beta_h(\boldsymbol{w},\boldsymbol{\varphi}). \tag{2.19}$$

($\equiv 0$ for inviscid flow)

*d) Approximation of the convective terms:*

$$\boldsymbol{B}_h(\boldsymbol{w}_h, \boldsymbol{\varphi}_h) = -\sum_{i\in I} \int_{K_i} \sum_{s=1}^{N} \boldsymbol{f}_s(\boldsymbol{w}_h) \cdot \frac{\partial \boldsymbol{\varphi}_h}{\partial x_s}\, \mathrm{d}x$$
$$+ \sum_{i\in I} \sum_{j\in S(i)} \int_{\Gamma_{ij}} \boldsymbol{H}(\boldsymbol{w}_h|_{\Gamma_{ij}}, \boldsymbol{w}_h|_{\Gamma_{ji}}, \boldsymbol{n}_{ij}) \cdot \boldsymbol{\varphi}_h \mathrm{d}S, \quad \boldsymbol{w}_h, \boldsymbol{\varphi}_h \in H^1(\Omega, \mathcal{T}_h)^m.$$

$\boldsymbol{H}(\alpha, \beta, \boldsymbol{n})$ = *numerical flux*:

– (locally) Lipschitz continuous
– consistent: $\boldsymbol{H}(\alpha, \alpha, \boldsymbol{n}) = \Sigma_{s=1}^{N} \boldsymbol{f}_s(\alpha) n_s$
– conservative: $\boldsymbol{H}(\alpha, \beta, \boldsymbol{n}) = -\boldsymbol{H}(\beta, \alpha, -\boldsymbol{n})$

## III) Treatment of boundary states

*a) Convective terms*

If $\Gamma_{ij} \subset \partial\Omega_h$, then there is no neighbour $K_j$ of $K_i$ adjacent to $\Gamma_{ij}$.
$\Longrightarrow$
$\boldsymbol{w}_h|_{\Gamma_{ji}}$ must be determined: we use *"inviscid" boundary conditions*

*b) The boundary state $\boldsymbol{w}_B = (w_{B1}, \ldots, w_{Bm})^{\mathrm{T}}$ in viscous terms*

sophisticated choice using the Dirichlet boundary conditions and extrapolation of the temperature on $\Gamma_I$ and of the density and temperature on $\Gamma_W$:

$$\begin{aligned} \boldsymbol{w}_B &= (\rho_{ij}, 0, \ldots, 0, \rho_{ij}\theta_{ij}) \quad \text{on } \Gamma_W, \\ \boldsymbol{w}_B &= \left(\rho_D, \rho_D v_{D1}, \ldots, \rho_D v_{DN}, \rho_{ij}\theta_{ij} + \frac{1}{2}\rho_D |\boldsymbol{v}_D|^2\right) \quad \text{on } \Gamma_I, \end{aligned}$$

$\rho_D$ and $\boldsymbol{v}_D = (v_{D1}, \ldots, v_{DN})$ – given density and velocity from the Dirichlet boundary conditions
$\rho_{ij}$, $\theta_{ij}$ – density and absolute temperature extrapolated from $K_i$ onto $\Gamma_{ij} \subset \partial\Omega_h$

**Approximate DGFE solution of the compressible Euler problem**: vector-valued function $\boldsymbol{w}_h$ such that

$$
\begin{array}{ll}
\text{a)} & \boldsymbol{w}_h \in C^1([0,T];\boldsymbol{S}_h) \\
\text{b)} & \dfrac{\mathrm{d}}{\mathrm{d}t}\left(\boldsymbol{w}_h(t),\boldsymbol{\varphi}_h\right) + \boldsymbol{B}_h\left(\boldsymbol{w}_h(t),\boldsymbol{\varphi}_h\right) = 0 \quad \forall\, \boldsymbol{\varphi}_h \in \boldsymbol{S}_h,\ t \in (0,T), \\
\text{c)} & \boldsymbol{w}_h(0) = \boldsymbol{w}_h^0,
\end{array}
$$

where $\boldsymbol{w}_h^0$ is an $\boldsymbol{S}_h$-approximation of $\boldsymbol{w}^0$.

**Approximate DGFE solution of the compressible Navier–Stokes problem**: vector-valued function $\boldsymbol{w}_h$ such that

$$
\begin{array}{ll}
\text{a)} & \boldsymbol{w}_h \in C^1([0,T];\boldsymbol{S}_h) \\
\text{b)} & \dfrac{\mathrm{d}}{\mathrm{d}t}\left(\boldsymbol{w}_h(t),\boldsymbol{\varphi}_h\right) + \boldsymbol{B}_h\left(\boldsymbol{w}_h(t),\boldsymbol{\varphi}_h\right) + \boldsymbol{A}_h\left(\boldsymbol{w}_h(t),\boldsymbol{\varphi}_h\right) = 0 \\
& \qquad\qquad\qquad\qquad\qquad\qquad \forall\, \boldsymbol{\varphi}_h \in \boldsymbol{S}_h,\ t \in (0,T), \\
\text{c)} & \boldsymbol{w}_h(0) = \boldsymbol{w}_h^0,
\end{array}
$$

where $\boldsymbol{w}_h^0$ is an $\boldsymbol{S}_h$-approximation of $\boldsymbol{w}^0$.

The DGFE problems are equivalent to large *systems of ordinary differential equations* which can be solved with the aid of a suitable ODE solver.

# 3 Some aspects of the DGFEM

## 3.1 Gibbs phenomenon and order limiting

Numerical solution of problems with zero or small viscosity suffer from spurious overshoots and undershoots near discontinuities or steep gradients = *Gibbs phenomenon*.

To cure this disease: *limiting of order of accuracy*

M.F., V. Dolejší and C. Schwab: new limiting method suitable in the framowork of the DGFEM based on the *jump indicator*

$$g(i) = \frac{\int_{\partial K_i} [\rho]^2 \,\mathrm{d}S}{h_i |K_i|^{3/4}}. \tag{3.20}$$

Applied in such a way that instead of $\boldsymbol{B}_h(\boldsymbol{w}_h(t), \boldsymbol{\varphi}_h)$ we use $\boldsymbol{B}_h(\bar{\boldsymbol{w}}_h(t), \boldsymbol{\varphi}_h)$, where

$$\bar{\boldsymbol{w}}_h|_{K_i} := \begin{cases} \pi_0 \boldsymbol{w}_h|_{K_i} & \text{if } g(i) > 1, \\ \boldsymbol{w}_h|_{K_i} & \text{otherwise,} \end{cases} \qquad K_i \in_h^{\mathrm{T}}, \tag{3.21}$$

and

$$\pi_0 \boldsymbol{w}_h|_{K_i} \in P_0(K_i), \;\; \pi_0 \boldsymbol{w}_h|_{K_i} = \frac{1}{|K_i|} \int_{K_i} \boldsymbol{w}_h \,\mathrm{d}\boldsymbol{x}. \tag{3.22}$$

**Example**: scalar equation

### 3.2 Approximation of boundary

If curved parts of $\partial\Omega$ are approximated in a piecewise linear way $\Longrightarrow$ vertices become nonphysical source of entropy

Cured by *superparametric elements*:
boundary element with one curved side $\approx$ image of the reference element $\hat{K}$ in a *bilinear mapping*

### 3.3 Accuracy of the method

a) **Theoretical analysis**:

Full systems describing compressible flow are rather complicated (e.g., the existence of the solution of is still an open problem)

$\Longrightarrow$

M.F., V.D., C. Schwab, V. Sobotíková:

theoretical analysis of the proposed numerical scheme was carried out for a *scalar nonlinear nonstationary convection-diffusion equation* equipped with Dirichlet boundary condition and initial condition:

$$\frac{\partial u}{\partial t} + \sum_{s=1}^{N} \frac{\partial f_s(u)}{\partial x_s} = \varepsilon \Delta u + g$$

The error $e_h = u_h - u$ satisfies the estimate

$$\sup_{t\in[0,T]} \|e_h(t)\|^2_{L^2(\Omega)} + \varepsilon \int_0^T \left( |e_h(\vartheta)|^2_{H^1(\Omega,\mathcal{T}_h)} + J_h^\sigma(e_h(\vartheta), e_h(\vartheta)) \right) \mathrm{d}\vartheta$$
$$\leq\ h^{2p} \left\{ C_1 \exp\left( C_2 \frac{1+\varepsilon}{\varepsilon} T \right) + C_3 \right\},$$

with constants $C_1, \ldots, C_3 > 0$ independent of $h$ and $\varepsilon$.

Error estimate – not optimal in $L^\infty(L^2)$-norm due to the technique required by the nonlinearity of the problem: *Young inequality, Gronwall lemma*

*Improvement* for a linear convection-diffusion-reaction problem:

M.F., K. Švadlenka: $\|e_h(t)\|_{L^2(\Omega)} = O(h^{p+1/2})$

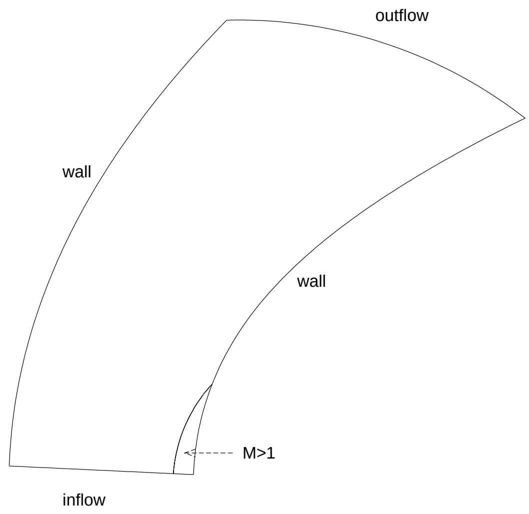


Figure 1: Geometry for Ringleb flow problem with marked supersonic region

## b) **Numerical experiments - experimental order of convergence (EOC)**

*Ringleb flow problem* =
an analytical smooth steady-state solution of the Euler equations obtained with the aid of the "hodograph method"
– represents a transonic channel flow, which is mostly subsonic, with a small supersonic region near the right-hand side wall, as shown in Figure 1.

The steady-state solution is achieved by a time stabilization method for "$t \to \infty$".

The computations performed on 4 triangular grids $T_{h_l}$, $l = 1, \ldots, 4$, having $5 \times 10$, $10 \times 20$, $20 \times 40$ and $40 \times 80$ vertices.

Computational error

$$E_h^2 \equiv \|\boldsymbol{w}_h - \boldsymbol{w}\|^2_{[L^2(\Omega_h)]^4} \approx C h^\alpha \tag{3.23}$$

| mesh | $E_h$ | $\alpha_l$ |
|---:|---|---|
| $5 \times 10$ | 7.85E-03 | – |
| $10 \times 20$ | 1.51E-03 | 2.05 |
| $20 \times 40$ | 3.41E-04 | 2.01 |
| $40 \times 80$ | 7.86E-05 | 2.04 |

Table 1: Computational errors $E_h$ in the $L^2$-norm and corresponding experimental order of accuracy $\alpha_l$

Experimental order of convergence given by

$$\alpha_l = \frac{\log\left(E_{h_l}/E_{h_{l-1}}\right)}{\log\left(h_l/h_{l-1}\right)}, \quad l = 2, \dots, 4, \tag{3.24}$$

where $h_l$ is the mesh size of $\mathcal{T}_{h_l}$.

### 3.4 Explicit $\times$ implicit discretization

forward Euler: severe CFL-stability condition $\Longrightarrow$ $\Delta t$ extremaly small

M.F., V.D.: 2 versions of semiimplicit method – linear problem on each time level – 10 times faster than the forward Euler

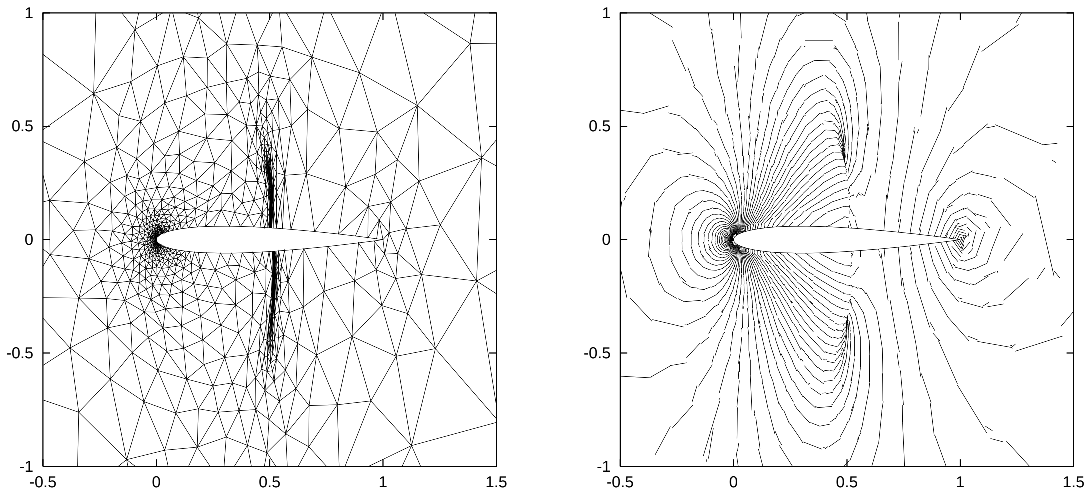

Figure 2: Inviscid flow along NACA 0012, $M_{\mathrm{in}} = 0.8$, zero angle of attack, triangulation (left) and isolines of the Mach number (right)

# 4 Applications

## 4.1 Euler equations

Inviscid flow around the profile NACA0012
a) far field Mach number $M_{\mathrm{in}} = 0.8$

zero angle of attack

computational mesh (number of triangles $\#\mathcal{T}_h = 1766$) obtained by the anisotropic mesh adaptation method
–sharp capturing of the shock wave
– no spurious oscillations, overshoots or undershoots

b) far field Mach number $M_{\mathrm{in}} = 0.8$

angle of attack $= 1.25°$

### 4.2 Navier-Stokes equations

Viscous flow around the profile NACA0012 with data from Bristeau, Glowinski, Periaux, Viviand: Numerical Simulation of Compressible Navier-Stokes Flows, Vieweg, 1987

| case | $M_{\text{in}}$ | $\alpha$ | $Re$ |
|---|---|---|---|
| C1 | 0.80 | 10° | 500 |
| C2 | 2.00 | 10° | 106 |
| C3 | 0.85 | 0° | 500 |
| C4 | 0.85 | 0° | 2000 |

Computed lift $c_L$ and drag $c_R$ coefficients in comparison with Bristeau et al. ($\#\mathcal{T}_h$ denotes the number of elements of the mesh $\mathcal{T}_h$)

| case | $\#_h^{\mathrm{T}}$ | computed values $c_L$ | $c_D$ | reference values $c_L$ range | $c_D$ range |
|---|---|---|---|---|---|
| C1 | 4563 | 0.4985 | 0.1938 | (0.4199 – 0.5170) | (0.1597 – 0.2868) |
| C2 | 5640 | 0.3969 | 0.4172 | (0.3063 – 0.4059) | (0.4120 – 0.4910) |
| C3 | 4946 | 0.0003 | 0.2304 | (0.0000 – 0.0007) | (0.1790 – 0.2420) |
| C4 | 4946 | 0.0001 | 0.1179 | (0.0000 – 0.0002) | (0.1012 – 0.1360) |

The computed values of drag and lift correspond to the reference values.

# 5 Conclusion

Theoretical results and numerical experiments show that DGFEM is a promising technique for the numerical solution of singularly perturbed problems with dominating convection, conservation laws and compressible flow.

*Further goals and open problems:*

– develop efficient implicit or semi-implicit schemes for the Navier-Stokes equations

– apply higher degree elements ($p > 1$)

– analyze symmetric and nonsymmetric formulations of diffusion terms in the framework of nonlinear convection-diffusion problems

– derive optimal error estimates

– develop a posteriori error estimates